CrossMark

RESEARCH PAPER

Characteristic seasonal variation in dissolved uranium concentration induced by the change of lake water pH in Lake Biwa, Japan

Akihito Mochizuki[1] · Ko Hosoda[1] · Masahito Sugiyama[1]

Abstract Epilimnion-dominated profiles of dissolved uranium (U) have been observed during summer in an oxygenated Japanese lake, Lake Biwa, contrary to the commonly accepted view that U shows conservative behavior in oxygenated seas and lakes. Monthly observations were conducted to reveal the mechanism for such characteristic distribution and geochemical behavior of dissolved U in the lake. In the surface water, dissolved U concentration started to increase in spring, peaked in summer, and decreased from autumn to winter. In contrast, the concentration remained almost constant in the middle layer (40 m depth) and decreased slightly in the bottom layer (70 m depth) throughout the stagnation period. Mass balance calculations of U suggest that the major mechanism for seasonal variations in the surface layer is the supply of U, not via water inflow from the watershed, but by internal chemical reactions within the lake. A laboratory experiment using the lake water and sediment demonstrated that U was desorbed from and adsorbed onto sediment in response to variations in lake water pH. From these results, it is inferred that the seasonal variation in the concentration of dissolved U in the epilimnion results mainly from the desorptive/adsorptive processes of U between sediment/water interface in response to variation in water pH, which is affected by biological activity in the lake.

✉ Masahito Sugiyama
sugiyama.masahito.5s@kyoto-u.ac.jp

[1] Graduate School of Human and Environmental Studies, Kyoto University, Yoshida-nihonmatsu-cho, Sakyo, Kyoto 606-8501, Japan

Introduction

The distribution and geochemical behavior of uranium (U) in aquatic environments have been investigated by many researchers. The interest in this subject is primarily attributable to the geoscientific significance of U as a tracer for dating various oceanographic processes (e.g., Broecker and Peng 1982) and estimating the sources of dissolved solutes in river basins (Chabaux et al. 2001, 2008; Ryu et al. 2009). In addition, investigations of naturally occurring U behavior within the hydrosphere, particularly in limnetic areas, have become more important recently because naturally occurring U can be useful as an analogue for predicting the transport and fate of anthropogenic U in natural waters following its release from nuclear materials and wastes.

U in oxygenated natural waters usually takes the form of a uranyl ion (UO_2^{2+}), which forms carbonate complexes such as $UO_2(CO_3)_2^{2-}$ and $UO_2(CO_3)_3^{4-}$ within a neutral or alkaline pH range (Langmuir 1978). Dissolved U shows vertically uniform distribution in oxygenated seawater (Ku et al. 1977; Delanghe et al. 2002) and lake water (Falkner et al. 1991) due to the good solubility of these complexes. In addition, the formation of calcium–uranyl-carbonate complexes [$CaUO_2(CO_3)_3^{2-}$ and $Ca_2UO_2(CO_3)_3^0$ (aq)] has also been suggested recently (Kalmykov and Choppin 2000; Bernhard et al. 2001). Thermodynamic calculations suggest that the $Ca_2UO_2(CO_3)_3^0$ (aq) complex may be the predominant aqueous species of dissolved U (IV) (Bernhard et al. 2001; Dong et al. 2005). Dong and Brooks (2006) found that not only calcium but also other alkaline

_Springer

earth metals (magnesium, strontium, and barium) form complexes with uranyl and carbonate ions. Those studies indicate that complexation with carbonate and alkaline earth metal ions, particularly calcium ions, is an important factor controlling the geochemical behavior of U in natural aquatic environments.

The geochemical behavior of U is also controlled by the redox condition of the water. Under strongly anoxic conditions, U (VI) can be reduced to U (IV). Since U (IV) tends to precipitate as insoluble species such as UO_2 (Langmuir 1978), a decrease of dissolved U concentration with depth can be observed in strongly reducing environments, such as the anoxic bottom water of the Black Sea (Anderson et al. 1989), the brine in the Mediterranean Sea (Van der Weijden et al. 1990), and pore water in oceanic littoral sediment (Klinkhammer and Palmer 1991).

An interesting distribution of dissolved U has been observed in the well-oxygenated, monomictic Lake Biwa in Japan. Dissolved U concentration in surface water during summer was approximately double that observed in bottom water (Takaku et al. 2003; Sakamoto et al. 2004). To the best of our knowledge, such an epilimnion-dominated distribution of dissolved U differs from the vertically homogeneous profiles observed in seawater (Ku et al. 1977; Delanghe et al. 2002) and lake water (Falkner et al. 1991), and has not been reported previously in oxygenated natural waters. The epilimnion-dominated distribution of dissolved U concentration can be interpreted as indicating either the removal of U from the bottom layer or supply to the surface layer (Sakamoto et al. 2004). However, the detailed mechanisms of such distribution are unknown, because U distribution throughout the year, and its mass balance in the lake, have not been established.

We previously reported the characteristic distribution of dissolved vanadium and tungsten in Japanese lakes including Lake Biwa (Sugiyama 1989; Harita et al. 2005). Similar to U, these elements also showed epilimnion-dominated distribution in summer, which was attributed to the desorptive/adsorptive processes between water/littoral sediment induced by the variation in lake water pH (Harita et al. 2005). Therefore, it is expected that the characteristic distribution of U in Lake Biwa results from a similar mechanism.

The present study found unexpected vertical profiles and seasonal variations of dissolved U concentration in Lake Biwa. In order to elucidate the mechanisms for this seasonal variation, we measured U concentration in the watershed of the lake and calculated its mass balance in the lake using our concentration data in combination with previously reported hydrological data. In addition, we investigated empirically the behavior of U between water and sediment. From these results, we propose desorption/adsorption of U from/onto the solid phase (i.e., sediment and suspended particulate matter) in response to variations in water pH as a likely mechanism for the seasonal variation in U concentration.

Studied lake

The characteristics of the study site are as follows (Somiya 2000). Lake Biwa is the largest lake in Japan, and is located at 35°15′N, 136°05′E. Geographically, it consists of northern and southern basins. The northern basin is the main basin and has a surface area of 616 km^2 and a capacity of 27.3 km^3. Its average and maximum depths are 43 and 104 m, respectively. In this basin, thermal stratification usually occurs from late April to early January (stagnation period), and vertical mixing of the lake water occurs regularly from late January to early April (circulation period). Although approximately 110 rivers flow into the northern basin, it has no direct outflow river; instead, water from the northern basin passes first into the southern basin.

The southern basin has a surface area of 58 km^2 and capacity of 0.2 km^3, with average and maximum depths of 3.5 and 8 m, respectively. Water in the southern basin outflows via one river (Seta River) and three channels (two Biwako-Sosui canals and Uji power plant canal) located in the basin.

Materials and methods

Sampling

We carried out monthly observations at Lake Biwa from February 2011 to February 2013. The sampling station was Ie-1 (73 m depth, 35°13′N, 136°00′E), located in the northern basin (Fig. 1). We collected water samples vertically using a Niskin water sampler. The samples were immediately filtered aboard the research vessel, using a 0.45-µm polyvinylidene fluoride filter Millex® (Millipore) attached to a polypropylene (PP) syringe. We washed the filter with the water sample before filtrating. We have confirmed that this filtration process does not contaminate filtrates. The filtrates were stored in low-density polyethylene (LDPE) bottles (Nalgene) and were acidified to pH 2 by adding ultrapure nitric acid (60 %, Kanto Kagaku). We measured WT and dissolved oxygen (DO) concentration using a multi-water quality profiler, ASTD-101 (JFE ALEC), and measured pH via the colorimetric method.

In order to estimate the input of U from the watershed, we sampled river, spring, and rain waters in or near the watershed of Lake Biwa. We sampled river waters flowing into the northern basin in May 2012 (14 rivers) and May 2013 (11 rivers). Based on the discharge data from

Fig. 1 Location of sampling stations. *1* Yasu River, *2* Hino River, *3* Echi River, *4* Uso River, *5* Inukami River, *6* Seri River, *7* Amano River, *8* Ane River, *9* Yogo River, *10* Ohura River, *11* Chinai River, *12* Ishida River, *13* Ado River, *14* Kamo River, *15* Ukawa River, *16* Wani River, *17* Wakamiya Spring, *18* Oe Spring, *19* Sansyaku Spring, *20* Kyoto University
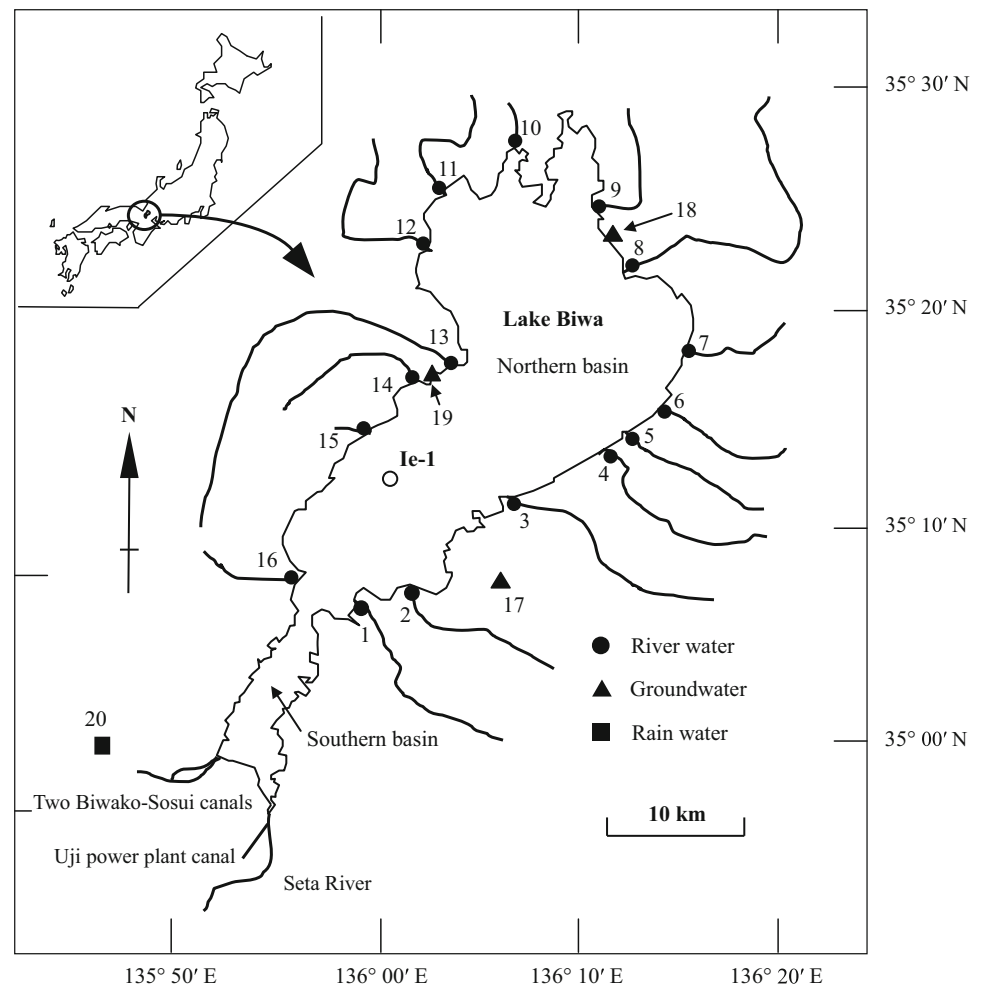
Kunimatsu ([1981](#)), the sum of the discharge of the rivers sampled in respective years accounts for 64 and 56 % of total riverine inflow to the northern basin. We also collected spring waters around the lake in May 2012 (1 spring) and May 2013 (3 springs). We assumed that the quality of water from these springs was the same as the groundwater flowing directly into the lake. Moreover, we collected rainwater twice during July 2012. We fixed a funnel to an LDPE bottle and placed it on the roof of a 30-m tall building (Kyoto University) located 7 km southwest of the lake. The amount of precipitation was calculated by the volume of the collected rainwater and the area of the funnel mouth. These water samples were filtered and acidified in the same way as the lake water. All the sampling sites are shown in Fig. [1](#).

All the equipment and vessels used for sampling, filtration, and storage (except for the Millex® filter) were previously cleaned by soaking them in 10 % Scat detergent (Nacalai Tesque) and 4 mol l^{-1} HNO$_3$ (Nacalai Tesque), followed by rinsing with purified water from a Milli-Q (Millipore) system (hereafter, MQW).

Analytical methods

The concentration of dissolved U in lake, river, spring, and rain waters was determined by inductively coupled plasma mass spectrometry (ICP–MS), using bismuth as an internal standard element (Mochizuki and Sugiyama [2012](#)). Into a polyethylene centrifuge tube contained 10 ml of either the sample or standard solution, 100 μl of bismuth stock solution and 100 μl of ultrapure nitric acid (60 %) were spiked.

The standard solution of U was prepared by diluting an ICP–MS multi-element standard of 10 mg-U l^{-1} (ICP–MS Quality Control Sample 2, Merck) to the desired concentration with the MQW. The internal standard bismuth stock solution was prepared by diluting a bismuth standard solution of 1 g l^{-1} (Wako Junyaku Kogyo) to 1 mg l^{-1} (4.8 μmol l^{-1}) with the MQW. We obtained the concentration of U in a sample solution using the ionic count ratio of ^{238}U/^{209}Bi, established via ICP–MS (Element 2, Thermo Fisher Scientific).

We evaluated the detection limit, accuracy, and precision of our method (Mochizuki and Sugiyama [2012](#)). The

detection limit of U was 1.6 pmol l^{-1} ($n = 10$, signal/noise ratio was 3.28). The U concentration in a certified reference material of river water (JSAC 0302-3, The Japan Society for Analytical Chemistry) was 13 ± 0.5 pmol l^{-1} ($n = 10$), which agreed with the certified value of 13 ± 0.4 pmol l^{-1} (3.1 ± 0.1 ng l^{-1}). The relative standard deviation for the measurement of 126 pmol l^{-1} (30.0 ng l^{-1}) U standard solution was 1.03 % ($n = 10$). We therefore concluded that our analytical method is reliable.

For the calculation of dissolved U speciation in the lake water, the concentrations of major cations (Na^+, K^+, Mg^{2+}, and Ca^{2+}) and major anions (Cl^-, SO_4^{2-}, and alkalinity) were also determined. Major cations were determined in lake water samples collected from February 2011 to December 2012. The concentrations of Na^+ and K^+ were determined via atomic adsorption spectrometry (AA-845, Japan Jarrel Ash), and those of Mg^{2+} and Ca^{2+} via inductively coupled plasma atomic emission spectrometry (Optima 5300DV, PerkinElmer). Since we rarely collected samples for anion determination (without acid addition), major anions were determined in lake water samples collected in May 2010 (only alkalinity), November 2011, May 2013 (only Cl^- and SO_4^{2-}), September 2013, and July 2014. The concentrations of Cl^- and SO_4^{2-} were determined via ion chromatography (L-7000 series, Hitachi and TSKgel IC-Anion-PW column, Tosoh), and alkalinity by acid titration (0.05 mol l^{-1} H_2SO_4) to pH 4.8 (Stumm and Morgan 1996).

Laboratory experiment

A laboratory experiment was conducted to investigate the effect of pH variation on the distribution of dissolved U

between lake water and sediment. A schematic of the experimental system is shown in Fig. 2. The system consisted of two parts: a water tank and gas controller. The tank (24 cm width, 16 cm depth, 28 cm height) contained approximately 1000 cm^3 of sediment collected on the boundary of the two lake basins (7 m depth). Ten liters of lake water collected from a depth of 40 m at Ie-1 was filtered through a 0.4-μm Nuclepore® filter (Whatman) and 0.1 mol sodium azide (NaN_3) was added to prevent biological activity. The water was then gently poured onto the sediment. The tank was kept in darkness at a constant temperature (25 °C). The pH of the lake water was controlled by bubbling carbon dioxide (CO_2) gas and CO_2-free air. The CO_2 gas was supplied by a cylinder and the CO_2-free air was prepared by passing natural air through 3 mol l^{-1} potassium hydroxide (KOH) solution and MQW. The pH value of the lake water was varied by controlling CO_2 pressure.

The experimental period (13 days) was divided into three sub-periods. In the first period (period 1; 0.0–4.0 days), the pH of lake water was maintained at approximately 7.0 (the value usually observed throughout the water column during the circulation period) by bubbling of CO_2 gas (5 ml min^{-1}) and CO_2-free air (1.5 l min^{-1}). In the second period (period 2; 4.0–10.2 days), pH was raised to around 8.5 (usually observed value in the epilimnion during summer) by bubbling CO_2-free air (1.5 l min^{-1}). In the third period (period 3; 10.2–13.0 days), the pH was decreased and maintained at 7.0 as in period 1. In each period, samples were collected 6, 12, and 6 times, respectively. In each sampling time, two aliquots of 25 ml sample water were taken from the tank by a PP syringe. The samples were immediately filtered using Millex®

Fig. 2 Schematic of experimental setup for the behavior of uranium between water and sediment
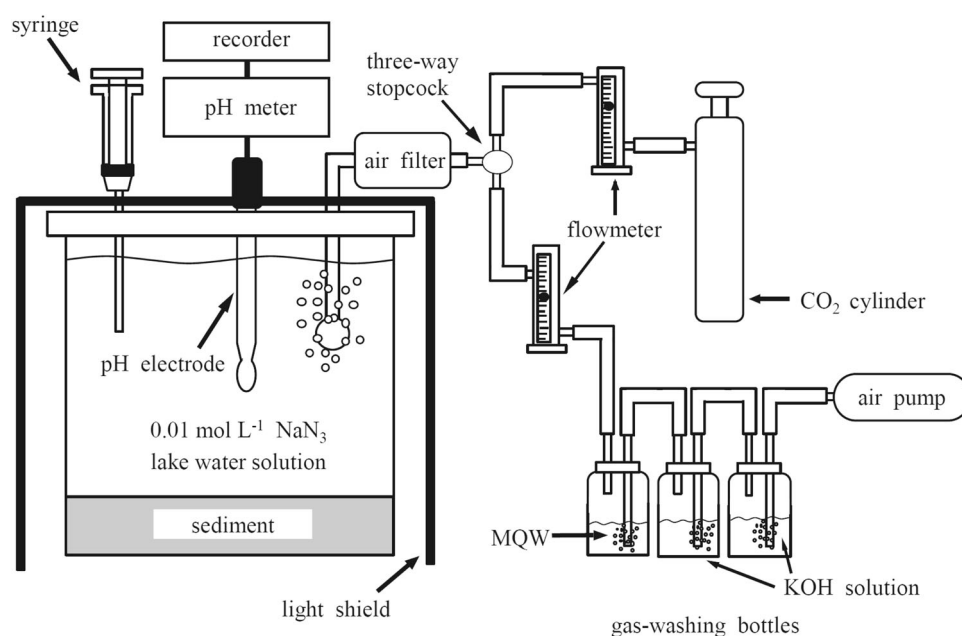
filters, and nitric acid was added to the filtrates. The concentrations of dissolved U in the samples were determined by the method described above.

Model calculation

In order to elucidate the mechanism for seasonal variation of U concentration in Lake Biwa, we calculated the daily mass balance of U in the lake during the stagnation periods. The model was applied only to the epilimnion of the northern basin and the following were assumed: (1) water from the watershed flows into the epilimnion but never directly into the hypolimnion, and outflow of lake water from the northern to the southern basin comes from the epilimnion of the northern basin alone; (2) lake water in the epilimnion and the hypolimnion are mixed by the daily change in depth of the thermocline during the stagnation period, but the water and chemical components do not diffuse across the thermocline; (3) dissolved U concentration is constant in the epilimnion within a given day, because the change in U mass in the epilimnion is homogenized quickly throughout the entire water layer.

Prior to estimating the U mass balance, we calculated the monthly balance of water flow. The balance throughout the entire lake (northern and southern basins) is represented as follows:

$$Q_{WR} + Q_{WG} + Q_{WP} = Q_{WO} + Q_{WE} + \Delta V_W, \qquad (1)$$

where Q_{WR}, Q_{WG}, and Q_{WP} represent the monthly inflow to the entire lake system from rivers, groundwater, and precipitation, respectively; Q_{WO} is the monthly discharge from the southern basin to the Seta River and three canals; Q_{WE} is the monthly evaporation rate; and ΔV_W is the monthly volume change of the lake water. The discharge to the Seta River, precipitation to the entire lake, and variation in water level for the entire lake are recorded daily by the Ministry of Land, Infrastructure, Transport, and Tourism (Biwako Office, Kinki Regional Development Bureau). In addition, average annual discharge from the three canals and average annual evaporation rate (Somiya 2000) and its monthly variation (Okamoto 1992) have been reported previously. Using these data together with the surface area of Lake Biwa (674 km^2), monthly values were calculated for Q_{WP}, Q_{WO}, Q_{WE}, and ΔV_W. By substituting these values in Eq. (1), we obtained monthly values for Q_{WR} and Q_{WG} in combination. From this total, the respective values for Q_{WR} and Q_{WG} were presumed to be proportional to their annual average flow rates (11.5:1.0; Somiya 2000).

Since our mass balance calculation is focused on the northern basin, the flow rates into the entire lake should be apportioned between the northern and southern basins. The monthly precipitation rate to the northern basin (Q_P), the monthly evaporation rate from the northern basin (Q_E), and

the monthly change of lake water volume in the northern basin (ΔV) were obtained via the surface area of the northern basin proportional to the entire lake (0.941) and the respective values of Q_{WP}, Q_{WE}, and ΔV_W. The monthly inflows to the northern basin via rivers (Q_R) and groundwater (Q_G) were calculated similarly, using the riverine flow rate into the northern basin relative to the entire lake (0.914) obtained by Kunimatsu (1981) and the respective values of Q_{WR} and Q_{WG}. The monthly transfer from the northern to the southern basin (Q_O) was calculated by substituting the above values into a water flow rate equation for the northern basin, represented as follows:

$$Q_R + Q_G + Q_P = Q_O + Q_E + \Delta V. \qquad (2)$$

Finally, each term in Eq. (2) was divided by the number of days in each month to obtain daily values. The daily inflow rate of river waters (Q_R'), groundwater (Q_G') and

Table 1 Daily inflow rate via river (Q_R'), groundwater (Q_G'), and precipitation (Q_P'); daily riverine outflow rate (Q_O'); and evaporation rate (Q_E') for the epilimnion of the northern basin during each month ($\times 10^9$ l day^{-1})

	Q_R'	Q_G'	Q_P'	Q_O'	Q_E'
2011					
Feb	12.4	1.08	2.96	10.4	0.940
Mar	17.4	1.52	2.06	19.9	0.701
Apr	11.5	0.998	2.54	10.6	0.147
May	27.1	2.36	7.61	30.9	0.042
Jun	13.6	1.19	2.64	31.9	0.130
Jul	12.4	1.08	4.34	16.2	0.970
Aug	4.22	0.367	1.87	7.51	1.13
Sep	33.5	2.91	9.50	42.8	1.70
Oct	8.09	0.703	2.74	8.63	1.50
Nov	6.25	0.543	1.97	7.34	1.22
Dec	6.06	0.527	2.51	7.14	1.17
2012					
Jan	9.06	0.788	2.19	11.1	1.16
Feb	13.5	1.18	2.97	17.0	0.908
Mar	19.7	1.72	3.08	22.9	0.701
Apr	18.3	1.59	2.41	17.3	0.147
May	6.48	0.564	1.87	10.3	0.042
Jun	16.6	1.45	5.40	29.5	0.130
Jul	18.5	1.61	5.15	24.5	0.970
Aug	5.75	0.500	2.44	9.16	1.13
Sep	6.12	0.532	5.21	10.8	1.70
Oct	14.3	1.25	1.84	15.3	1.50
Nov	7.14	0.621	2.95	6.82	1.22
Dec	9.92	0.863	3.04	9.28	1.17
2013					
Jan	11.1	0.962	2.07	16.3	1.16
Feb	13.0	1.13	2.96	13.6	0.940

precipitation (Q_P'), the daily outflow rate (Q_O'), and the daily evaporation rate (Q_E') are listed in Table 1.

Using these rates and observed U concentrations, we simulated the U concentration change in the epilimnion during the stagnation period, from May to the following January, in 2011 and 2012. As shown in Fig. 3, daily change in the mass of dissolved U t days after the beginning of the calculation (ΔU_t; t represents natural numbers) is balanced to U input from riverine (U_R), groundwater (U_G), and precipitation inflow (U_P), U supply from the hypolimnion (U_H; $U_H \leq 0$ indicates the removal of U from the epilimnion to the hypolimnion), U supply from sediment in contact with the epilimnion (U_S; $U_S \leq 0$ indicates the removal of U from the lake water to the sediment), and U output to the southern basin (U_O). Therefore, the daily mass balance of U in the epilimnion during the stagnation period can be represented by the following:

$$\Delta U_t = U_R + U_G + U_P + U_H + U_S - U_O. \tag{3}$$

In Eq. (3), ΔU_t is transformed as follows:

$$\Delta U_t = [U]_t \times V_{Et} - [U]_{t-1} \times V_{E(t-1)}, \tag{4}$$

where $[U]_t$ and V_{Et} represent the simulated concentration of dissolved U and the calculated volume of the epilimnion of the northern basin t days after the beginning of the calculation, respectively. The U concentrations on the first day of the modeling ($[U]_0$) were assumed to be 76 pmol l^{-1} on 12 May 2011 and 99 pmol l^{-1} on 16 May 2012, based on the observed concentrations at 0 m depth. We also assumed that the thickness of the epilimnion varied linearly from day to day according to the monthly observed values, and V_{Et} was obtained daily based on the thickness of the epilimnion and a depth–volume diagram of Lake Biwa

Table 2. Similarly, U_R, U_G, and U_P in Eq. (3) can be transformed as follows:

$$U_R = [U]_R \times Q_R' \tag{5}$$

$$U_G = [U]_G \times Q_G' \tag{6}$$

$$U_P = [U]_P \times Q_P', \tag{7}$$

where $[U]_R$, $[U]_G$, and $[U]_P$ represent the average U concentration in river water, groundwater, and precipitation flowing into the northern basin, respectively (calculated in the following section). U_H in Eq. (3) can be transformed in two ways according to the daily volume change of the epilimnion. When the volume of the epilimnion increases ($V_{Et} > V_{E(t-1)}$; Fig. 3a), it can be transformed as follows:

$$U_H = [U]_H \times (V_{Et} - V_{E(t-1)}), \tag{8}$$

where $[U]_H$ represents the U concentration in the hypolimnion. We assumed that $[U]_H$ from 12 May 2011 to 25 January 2012 was the same as the average U concentration in the hypolimnion on 12 May 2011 (69 pmol l^{-1}), and that from 16 May 2012 to 16 January 2013 it was the same as that on 16 May 2012 (80 pmol l^{-1}). Conversely, when the volume of the epilimnion decreases ($V_{Et} < V_{E(t-1)}$; Fig. 3b), U_H can be transformed as follows:

$$U_H = [U]_{t-1} \times (V_{Et} - V_{E(t-1)}). \tag{9}$$

The value of U_S in Eq. (3) will be discussed in the following section. Finally, U_O in Eq. (3) is transformed as follows:

$$U_O = [U]_{t-1} \times Q_O' \tag{10}$$

When the thickness of the epilimnion increases, Eq. (3) can be transformed by using Eqs. (4–10) as follows:

$$[U]_t = \frac{[U]_R + Q_R' + [U]_G \times Q_G' + [U]_P \times Q_P' + [U]_H \times (V_{Et} - V_{E(t-1)}) + U_S - [U]_{t-1} \times Q_Q' + [U]_{t-1} \times V_{E(t-1)}}{V_{Et}} \tag{11}$$

produced by Okamoto (1992). The thickness and volume of the epilimnion on the observation days are shown in

Conversely, when the thickness of the epilimnion decreases, Eq. (3) can be transformed as follows:

$$[U]_t = \frac{[U]_R + Q_R' + [U]_G \times Q_G' + [U]_P \times Q_P' + [U]_{t-1} \times V_{Et} + U_S - [U]_{t-1} \times Q_O'}{V_{Et}} \tag{12}$$

Fig. 3 Schematic of uranium mass balance calculation for **a** stagnation period with increasing epilimnion volume and **b** stagnation period with decreasing epilimnion volume. ΔU_t daily change in mass of dissolved uranium t days after the beginning of the calculation, U_R uranium input from rivers, U_G uranium input from groundwater, U_P uranium input from precipitation, U_S uranium input to/output from the sediment, U_O uranium output to the southern basin, U_H uranium input to/output from the hypolimnion
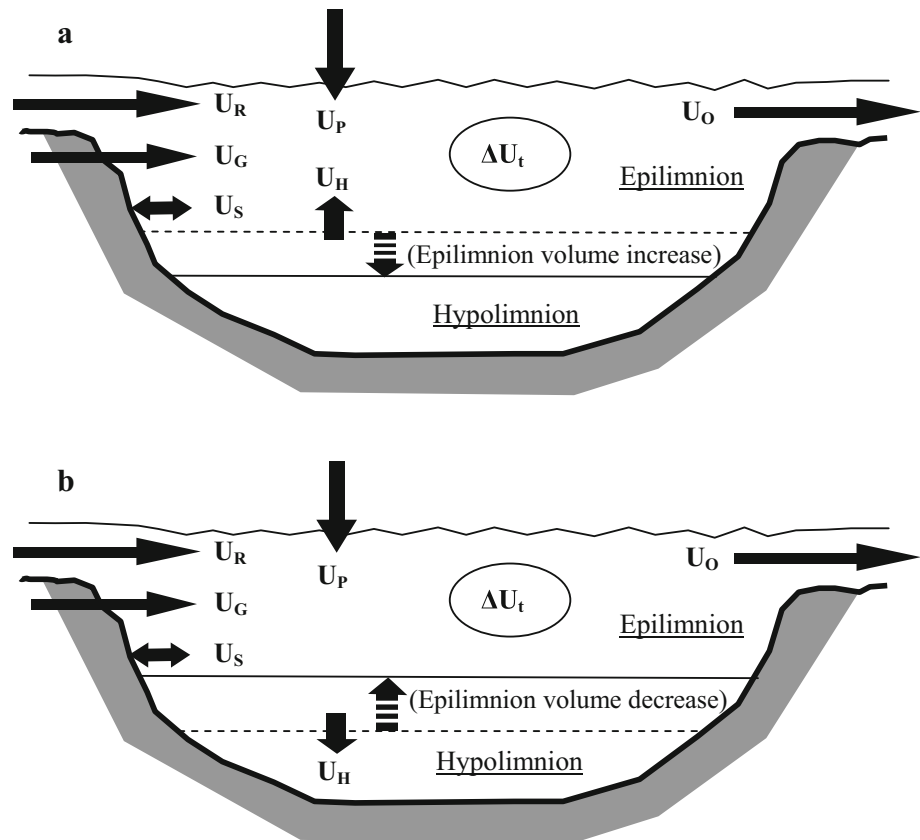
Using Eqs. (11) and (12), the daily values were calculated for $[U]_t$ during the stagnation period and compared with the U concentration measured at 0 m depth.

Results

Seasonal variations and vertical profiles in Lake Biwa

Seasonal variations in dissolved U concentrations at 0, 40, and 70 m depths at station Ie-1 are shown in Fig. 4. The data indicate that dissolved U concentration in the epilimnion of the northern basin shows a periodic variation: at 0 m depth, U concentration started to increase in spring, peaked in summer, and then decreased in autumn and winter. The minimum and maximum concentrations of U in 2011 were observed in February (65 pmol l^{-1}) and September (139 pmol l^{-1}), while those in 2012 were observed in February (75 pmol l^{-1}) and August (152 pmol l^{-1}), respectively. In contrast, dissolved U concentration at 40 m depth remained almost constant during the stagnation period and abruptly increased in January in both years, whereas that at 70 m depth gradually decreased during the stagnation period and showed an increase in February 2012

and January 2013. In general, U concentration at 40 m depth was greater than that at 70 m depth throughout the observation period.

WT, pH, and DO concentrations observed at 0 m and 70 m depth are listed in Table 3, together with dissolved U concentrations. Similar to the U concentration, WT and pH at 0 m depth showed an increase from spring to summer and a decrease from autumn to winter. The pH values at 0 m depth during summer were considerably higher in 2012 than in 2011. The values of WT at 70 m depth were almost constant throughout the 2 years, while those of DO concentration and pH decreased during the stagnation period and then increased in the following January or February. At 70 m depth, the minimum DO concentration and saturation ratio during the observation period were recorded in January 2012 (135 µmol l^{-1} and 36 % saturation, respectively).

Vertical profiles for WT, pH, DO concentration, and dissolved U concentration in February, May, September, and November 2011 are shown in Fig. 5. All four variables showed vertically uniform distributions in February 2011 (Fig. 5a, e, i, m). The profiles of these variables were also vertically constant in March and April 2011, February and March 2012, and January and February 2013 (data not shown). As also shown in Fig. 4 and Table 3, WT, pH, and dissolved U concentration in the epilimnion were greater

Table 2 Thickness and volume of epilimnion at Ie-1 on observation days

	Thickness (m)	Volume ($\times 10^{12}$ l)
2011		
10 Feb	73	25.7
1 Mar	73	25.7
5 Apr	73	25.7
12 May	12	6.39
7 Jun	7.0	3.83
5 Jul	5.0	2.77
2 Aug	5.0	2.77
15 Sep	5.0	2.77
18 Oct	19	9.73
14 Nov	20	10.2
12 Dec	21	10.6
2012		
25 Jan	53	21.8
28 Feb	73	25.7
27 Mar	73	25.7
17 Apr	73	25.7
16 May	13	6.89
12 Jun	7.5	4.10
3 Jul	7.0	3.83
1 Aug	6.0	3.30
12 Sep	11	5.89
16 Oct	18	9.04
13 Nov	25	12.4
12 Dec	32	15.1
2013		
16 Jan	73	25.7
19 Feb	73	25.7
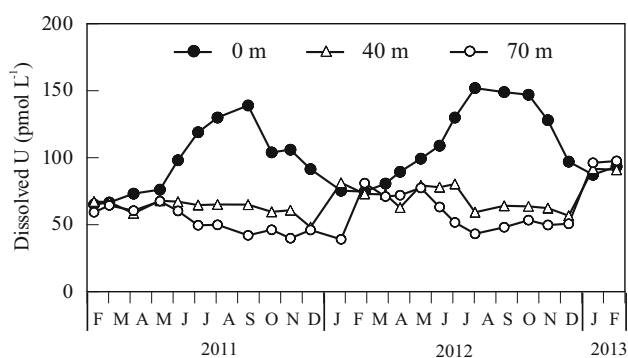
Fig. 4 Seasonal variation in dissolved uranium concentration at Ie-1 from February 2011 to February 2013

than those in the hypolimnion during May, September, and November 2011 (Fig. 5b–d, f–h, n–p). In addition, it is apparent from Fig. 5 that the remarkable changes in U concentration, WT, and pH occurred at the depth of the

thermocline. The DO concentration during the stagnation period showed a completely different distribution pattern from those for the other three variables: it decreased near the thermocline and at the bottom, particularly in September and November (Fig. 5k, l).

U concentrations in the watershed of Lake Biwa

U concentrations in river, spring, and rain waters in the Lake Biwa watershed are shown in Table 4. The concentration in river waters ranged from 13 pmol l^{-1} (Ishida River) to 952 pmol l^{-1} (Ukawa River). The water-discharge-weighted average concentration of U for river water ($[U]_R$) was calculated as 184 pmol l^{-1} using the U concentrations determined in this study and water discharge data reported for each river (Kunimatsu 1981). Mito et al. (2004) determined U concentration in 14 rivers flowing into the northern basin from April 1996 to June 1998. They reported the water-discharge-weighted average concentration as 152 pmol l^{-1}, which was broadly similar to our result. Sakamoto et al. (2004) also determined U concentration in 13 rivers in May, July, and November 2001. On the basis of their concentration data and the discharge data of Kunimatsu (1981), we calculated the water-discharge-weighted average values in the respective months as 106, 104, and 89 pmol l^{-1}, which did not show clear seasonal variation.

U concentrations in three spring waters were 3 pmol l^{-1} (Wakamiya Spring; the average of two samples collected in 2012 and 2013), 6 pmol l^{-1} (Oe Spring), and 2 pmol l^{-1} (Sansyaku Spring). The arithmetic average concentration of these spring waters ($[U]_G$) was 4 ± 2 pmol l^{-1}.

The concentrations in rainwater samples were 5 pmol l^{-1} (16 July 2012; precipitation was 3.8 mm) and 3 pmol l^{-1} (20 July 2012; precipitation was 3.1 mm). The precipitation-weighted average concentration of U in rain waters ($[U]_P$) was 4 pmol l^{-1}.

Experimental variation in U concentration

A laboratory experiment was conducted to examine the effects of pH on U distribution between water and sediment, using the setup shown in Fig. 2. The variation in pH observed in the experiment is shown in Fig. 6a, and the average U concentration of two samples collected simultaneously is shown with an error bar (standard deviation) in Fig. 6b. These results show that dissolved U concentration varied according to water pH. During period 1, the dissolved U concentration was almost constant (77 ± 12 pmol l^{-1}); during period 2, it increased in response to the higher pH; and during period 3, pH decreased to 7.0 and dissolved U concentration also decreased. In addition, it appears that the changes in U concentration lagged behind the changes in pH.

Table 3 Water temperature, pH, dissolved oxygen, and U concentrations at Ie-1

	0 m depth				70 m depth			
	WT (°C)	pH	DO (μmol l^{-1})	U (pmol l^{-1})	WT (°C)	pH	DO (μmol l^{-1})	U (pmol l^{-1})
2011								
10 Feb	7.5	7.1	377	65	7.6	7.1	338	59
1 Mar	7.7	7.2	363	67	7.2	7.1	346	64
5 Apr	8.7	7.3	355	73	7.8	7.1	352	61
12 May	13.9	7.3	333	76	7.6	7.0	298	68
7 Jun	19.1	7.7	314	98	7.6	7.0	295	60
5 Jul	24.7	7.9	288	119	7.6	6.9	275	50
2 Aug	26.5	8.0	263	130	7.6	6.9	246	50
15 Sep	27.2	7.8	269	139	7.6	6.8	175	42
18 Oct	20.4	7.4	279	104	7.7	6.8	181	46
14 Nov	17.8	7.4	299	106	7.8	6.8	146	40
12 Dec	12.4	7.2	306	92	7.8	6.8	179	46
2012								
25 Jan	8.4	7.2	335	75	7.8	6.8	135	39
28 Feb	7.1	7.1	383	75	7.1	7.0	340	81
27 Mar	7.6	7.2	363	81	7.3	7.1	342	71
17 Apr	10.9	7.3	352	90	7.6	7.1	334	72
16 May	14.8	7.4	324	99	7.4	7.0	314	78
12 Jun	20.3	8.5	328	109	7.4	7.0	267	63
3 Jul	22.9	9.6	354	130	7.4	7.0	252	52
1 Aug	28.8	9.6	245	152	7.4	6.8	193	43
12 Sep	28.0	7.9	239	149	7.5	6.6	149	48
16 Oct	20.9	7.4	268	147	7.6	6.8	185	53
13 Nov	16.1	7.4	297	128	7.6	6.9	182	50
12 Dec	10.9	7.2	337	97	7.6	6.7	168	51
2013								
16 Jan	8.2	7.2	318	87	8.1	7.2	321	96
19 Feb	6.9	7.2	395	94	7.0	7.1	360	98

Using the U concentrations, the water volume, and the bottom area of the water tank (384 cm^2) in the experiment, the rates of U release (4.0–6.1 days) and assimilation (10.2–11.9 days) were calculated as 1.86×10^4 and 2.76×10^4 pmol m^{-2} day^{-1}, respectively.

Discussion

In the northern basin of Lake Biwa, the dissolved U concentration at 0 m depth increased from spring to summer and decreased from autumn to winter (Fig. 4). In addition, Fig. 5 indicates that such seasonal variation in U concentration is restricted to the epilimnion. It is inferred from these results that U is supplied to the epilimnion from spring to summer, but is removed from autumn to winter. In contrast, U concentration at 40 m depth was almost constant during the stagnation period, whereas the concentration at 70 m depth decreased during the stagnation period in 2011 and from May to August in 2012. These findings suggest a process of removal of dissolved U at the bottom of the water column during the stagnation period. However, it is likely that the seasonal variation in U concentration within the epilimnion during the stagnation period is independent of such removal processes operating at the bottom. Therefore, in this paper, we will focus our discussion on the behavior of U in the epilimnion, and mechanisms for the removal processes at the bottom will be addressed in future studies.

Speciation of dissolved U in the lake water

In order to discuss the geochemical behavior of dissolved U in the lake, the chemical species of the U in the lake water was estimated using chemical thermodynamic computation software MINEQL+ (ver. 4.6; Schecher and
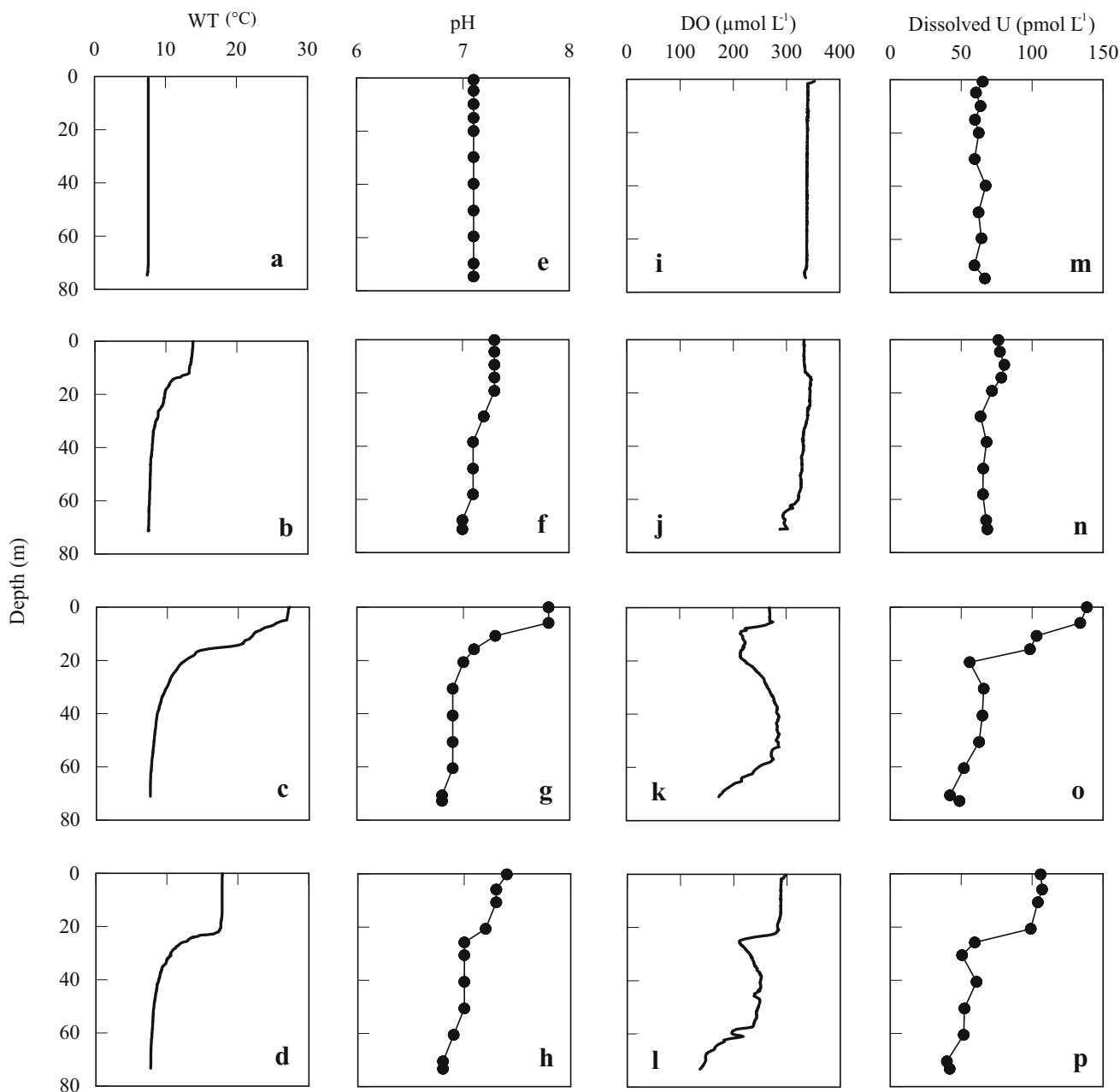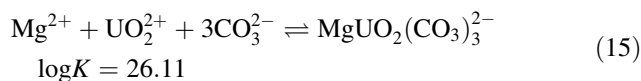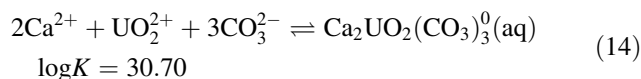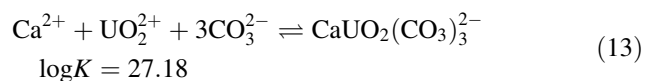
Fig. 5 Vertical profiles of water temperature (**a**, **b**, **c**, **d**), pH (**e**, **f**, **g**, **h**), dissolved oxygen concentration (**i**, **j**, **k**, **l**), and dissolved uranium concentration (**m**, **n**, **o**, **p**) at Ie-1 in February (**a**, **e**, **i**, **m**), May (**b**, **f**, **j**, **n**), September (**c**, **g**, **k**, **o**), and November (**d**, **h**, **l**, **p**) 2011

McAvoy 2006) and its database. The calcium–uranyl-carbonate species [$CaUO_2(CO_3)_3^{2-}$ and $Ca_2UO_2(CO_3)_3^0$ (aq)] and the magnesium–uranyl-carbonate species [$MgUO_2(CO_3)_3^{2-}$] were also included into the estimation using the formation constants of these species [shown in reactions (13–15)] by Dong and Brooks (2006).

$$Ca^{2+} + UO_2^{2+} + 3CO_3^{2-} \rightleftharpoons CaUO_2(CO_3)_3^{2-} \\ \log K = 27.18 \tag{13}$$

$$2Ca^{2+} + UO_2^{2+} + 3CO_3^{2-} \rightleftharpoons Ca_2UO_2(CO_3)_3^0(aq) \\ \log K = 30.70 \tag{14}$$

$$Mg^{2+} + UO_2^{2+} + 3CO_3^{2-} \rightleftharpoons MgUO_2(CO_3)_3^{2-} \\ \log K = 26.11 \tag{15}$$

For the calculation of U speciation in the lake, the concentrations of major ions at 0 m depth were determined. The minimum, maximum, and mean values and the relative

Table 4 Uranium concentrations in river waters, spring waters, and rain waters in the Lake Biwa watershed (pmol l^{-1})

	2012	2013	Average
River water			
Yasu	160	173	166
Hino	327	477	402
Echi	139	–	139
Uso	236	500	368
Inukami	172	–	172
Seri	468	446	457
Amano	359	430	395
Ane	167	182	174
Yogo	85	–	85
Ohura	373	529	451
Chinai	110	132	121
Ishida	13	–	13
Ado	25	30	28
Kamo	154	–	154
Ukawa	–	952	952
Wani	–	535	535
Spring water			
Wakamiya	4	3	3
Oe	–	6	6
Sansyaku	–	2	2
Rain water			
16 July	5	–	5
20 July	3	–	3

standard deviations are shown in Table 5. Although the number of samples for major anions ($n = 4$) is smaller than that of cations ($n = 23$), the concentration ranges were narrow and the relative standard deviations were small (at most 5.5 %) for all major ions, which indicates that their concentration was almost constant throughout the year. The constancy of major ion concentrations in the lake has also been reported by Fujinaga and Hori (1982), Mito et al. (2004), and Sugiyama et al. (2005). Therefore, we assumed that the values in Table 5 are representative of the average concentrations of major ions in the lake. Using these values and the average U concentration at 0 m depth (103 pmol l^{-1}), the relationship between the water pH and U species was calculated.

The result of this calculation is shown in Fig. 7. Within the pH range of 7–10, the predominant U species is $CaUO_2(CO_3)_3^{2-}$. At pH 7.0 both $Ca_2UO_2(CO_3)_3^0$ (aq) and $UO_2(CO_3)_2^{2-}$ are also major species, but with pH increase, the percentage of $Ca_2UO_2(CO_3)_3^0$ (aq) increases while that of $UO_2(CO_3)_2^{2-}$ decreases. Precipitation of calcite occurs at pH 8.7, and the predominance of $CaUO_2(CO_3)_3^{2-}$ over other U species becomes greater at pH > 8.7. The formation of
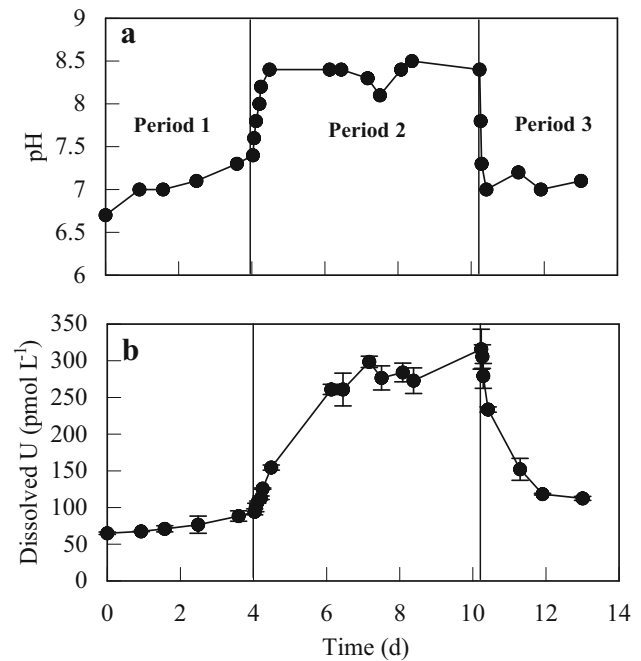
Fig. 6 Changes in **a** pH and **b** dissolved uranium concentration in lake water during the laboratory experiment. The *error bars* in **b** represent one standard deviation of the concentrations for two samples collected at the same time

$UO_2CO_3^0$ (aq) is negligible, and $UO_2(CO_3)_3^{4-}$ and $MgUO_2(CO_3)_3^{2-}$ are minor species within the pH range.

Since the changes in enthalpy and entropy of the formation of the calcium–uranyl-carbonate complexes are not known, the formation constants of these complexes at other temperatures cannot be estimated accurately. However, during summer and autumn, when water temperature is around 25 °C, the effect of water temperature on U speciation is small and therefore the predominant species is probably $CaUO_2(CO_3)_3^{2-}$. In addition, Wang et al. (2004) expected that the lowering of water temperature from 25 to 0 °C and subsequent changes in the formation constants of U species would not change the order of their percent distribution. Therefore, in the following section we assumed that the predominant aqueous U species was $CaUO_2(CO_3)_3^{2-}$.

Effect of water flow and epilimnion volume on U concentration

It was presumed that the major input of U to the epilimnion of the northern basin was the water flow from its watershed, particularly from rivers. In Lake Biwa and its surrounding area, the average U concentration in river waters ($[U]_R$; 184 pmol l^{-1}) is much higher than that in groundwater ($[U]_G$; 4 pmol l^{-1}), rain water ($[U]_P$; 4 pmol l^{-1}), and even than the concentration in lake waters at 0 m depth

Table 5 Major ion concentrations in Lake Biwa at 0 m depth

	Minimum	Maximum	Average	RSD (%)[c]
Major cations[a]				
Na$^+$ (µmol l^{-1})	293	364	322	5.5
K$^+$ (µmol l^{-1})	35.6	40.3	38.0	4.0
Mg^{2+} (µmol l^{-1})	78.8	96.5	90.0	3.8
Ca^{2+} (µmol l^{-1})	285	310	296	2.1
Major anions[a]				
Cl$^-$ (µmol l^{-1})	247	256	253	0.94
SO$_4^{2-}$ (µmol l^{-1})	77.4	81.6	79.8	1.8
Alkalinity (µeq l^{-1})[b]	696	712	705	2.2

[a] Major cations were determined monthly from February 2011 to December 2012, while major anions were determined irregularly (Cl$^-$ and SO$_4^{2-}$: November 2011, May and September 2013, and July 2014, alkalinity: May 2010, November 2011, September 2013, and July 2014)

[b] Alkalinity = [HCO$_3^-$] + 2[CO$_3^{2-}$] + [OH$^-$] − [H$^+$]

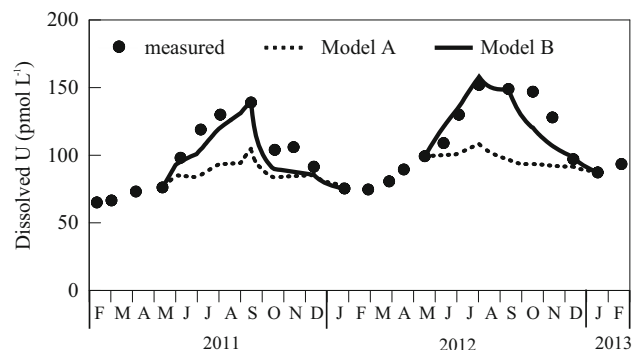[c] RSD denotes the percentage of standard deviation in the average concentration

Fig. 8 Time series (2011–2013) of dissolved uranium concentration measured at 0 m depth and concentrations in the epilimnion estimated by models A and B

Fig. 7 Aqueous uranium speciation as a function of pH within **a** pH 7.0–10.0 and **b** pH 8.5–10.0. Average of uranium concentration (103 pmol l^{-1}) and major ion concentrations shown in Table 5 were used for the calculation

during the circulation periods (65–94 pmol l^{-1}; Table 3). In addition, it has been reported that the annual discharge of rivers into the lake is approximately 10 times more than

that from groundwater and twice that of direct precipitation (Somiya 2000). On the basis of these findings, it was inferred that the input from river waters to the epilimnion increases the concentration of U in Lake Biwa from spring to summer. In contrast, from autumn to winter, deepening of the thermocline and subsequent increased volume of the epilimnion can dilute the U concentration in the epilimnion. Thus, we estimate the effect of water inflow as well as the water volume of the epilimnion on the U concentration in the epilimnion of the northern basin during the stagnation periods, using mass balance Eqs. (11) and (12). In this model (model A), we set the value of U$_S$ (Eqs. (11, 12)) as 0 in order to isolate the effects of water inflow and water volume on U concentration.

The results obtained via model A are shown by dotted lines in Fig. 8, together with the measured U concentrations at 0 m depth. The simulated U concentrations cannot account for the observed concentration changes during the stagnation periods. These results suggest that the inflow of dissolved U from the watershed and the volume change of

the epilimnion are not the major mechanism for the seasonal variation of U concentration in the epilimnion. Therefore, it is inferred that the epilimnion is subject to other major inputs of U from spring to summer and outputs from autumn to winter.

Effect of pH on the distribution of U between water and sediment

It is remarkable that dissolved U concentration in the epilimnion of the northern basin varies in response to changes in pH (Table 3). In addition, the vertical profiles of U concentration are similar to those of pH (Fig. 5). From these results, a relationship is suggested between the lake water pH and U concentration.

Various experimental studies have revealed the adsorptive behavior of uranyl-carbonate species between water and solids (Ishibashi et al. 1967; Hsi and Langmuir 1985; Ho and Miller 1986; Waite et al. 1994; Pabalan and Turner 1997; Barnett et al. 2002), and recently that of calcium–uranyl-carbonate species has also been discussed (Fox et al. 2006; Stewart et al. 2010). Most of these studies exhibited the desorption of U from ferric (oxy)hydroxides, aluminosilicates, or clay minerals from neutral to alkaline pH region. Such desorption of U can be explained by the formation of highly soluble uranyl-carbonate and calcium–uranyl-carbonate species, which results from the increase in water pH and subsequent increase in carbonate ion concentration. In Lake Biwa, a large fraction of sediments contain oxides and hydroxides of iron (3.3–5.2 % as iron content in the upper 2-cm layer; Takamatsu et al. 1985) and aluminosilicates or clay minerals (26.2 % as silicon content and 7.4 % as aluminum content in the upper 5-cm layer; Somiya 2000). Therefore, it is possible that the variation in lake pH from neutral to alkaline affects U speciation and its distribution between the lake water and the solid phase, resulting in the seasonal variation in dissolved U concentration.

We investigated this possibility experimentally, using the lake water and sediments (Fig. 2). The results (Fig. 6) showed that the U concentration in water increased with pH from 7.0 to 8.5, which is in agreement with the findings of previous experimental studies mentioned above. In addition, the result also indicates that the reaction of U in response to pH change is reversible: its concentration decreased with pH from 8.5 to 7.0 (Fig. 6). In this experiment, biological activity and change in WT had negligible effect on U concentration, because we filtered the lake water, added NaN_3 to it, and kept the tank in darkness at a constant temperature. The change in U concentration observed in our experiment is also evidently a result of chemical reactions between water and sediment in response to pH change. A similar reaction is expected to occur in the

epilimnion of the lake, resulting in the seasonal variation in dissolved U concentration.

From the above results, we propose a likely mechanism for the seasonal variation in dissolved U concentration (Fig. 9), as follows. During the circulation period, U is adsorbed onto minerals contained in the solid phase within a neutral pH range. As pH in the epilimnion increases due to biological activity from spring to summer, U is desorbed from the surface of sediment in contact with the epilimnetic lake water (defined as "littoral sediment") and suspended particulate matter in the epilimnion, thereby becoming concentrated within the epilimnion (Fig. 9a). Conversely, as pH in the epilimnion decreases due to the decline in biological activity in autumn, U in the epilimnion is adsorbed onto the surface of the solid phase in the epilimnion, and its concentration decreases (Fig. 9b).

In order to evaluate the possibility of this mechanism, we calculated the mass balance of U in the epilimnion of the northern basin, including the desorption/adsorption of U from/onto sediment (model B, $U_s \neq 0$ in Eqs. 11 and 12). We assumed that U was desorbed from the littoral sediment from 13 May to 15 September in 2011 and from 17 May to 12 September in 2012, along with the pH increase from spring to summer (Table 3). The daily value of U_S in these periods was obtained by multiplying the surface area of sediment in contact with the epilimnion by the desorption rate of U. The surface area of sediment was calculated daily using the thickness of the epilimnion and the depth–bathymetric area diagram of Lake Biwa from Horie (1961). The desorption rate was estimated in such a way that the simulated U concentration fits to the measured concentrations at 0 m depth on 15 September 2011 and 12 September 2012, respectively. We assumed that the desorption rates in 2011 and 2012 were independent of each other, but that each of them was constant throughout the respective period.

Conversely, we inferred that U in the epilimnion was adsorbed onto sediment from 16 September 2011 to 25 January 2012 and from 13 September 2012 to 16 January 2013, along with the pH decrease from autumn to winter (Table 3). The daily value of U_S was determined by the surface area of sediment and the adsorption rate. The surface area of sediment was determined in the same way as described above, and the adsorption rate was estimated in such a way that the simulated U concentration fits to the measured concentrations at 0 m depth on 25 January 2012 and 16 January 2013, respectively.

The results (Fig. 8) show that the U concentration simulated by model B is in good agreement with the measured value from spring to summer, but is slightly lower from autumn to winter. The estimated desorption rate from May to September was 2.50×10^4 pmol m^{-2} day^{-1} in 2011 and 4.80×10^4 pmol m^{-2} day^{-1} in 2012, and the estimated adsorption rates from September to the following January

Fig. 9 Likely mechanism for **a** increase and **b** decrease of dissolved uranium concentration in the epilimnion

a From spring to summer

b From autumn to winter
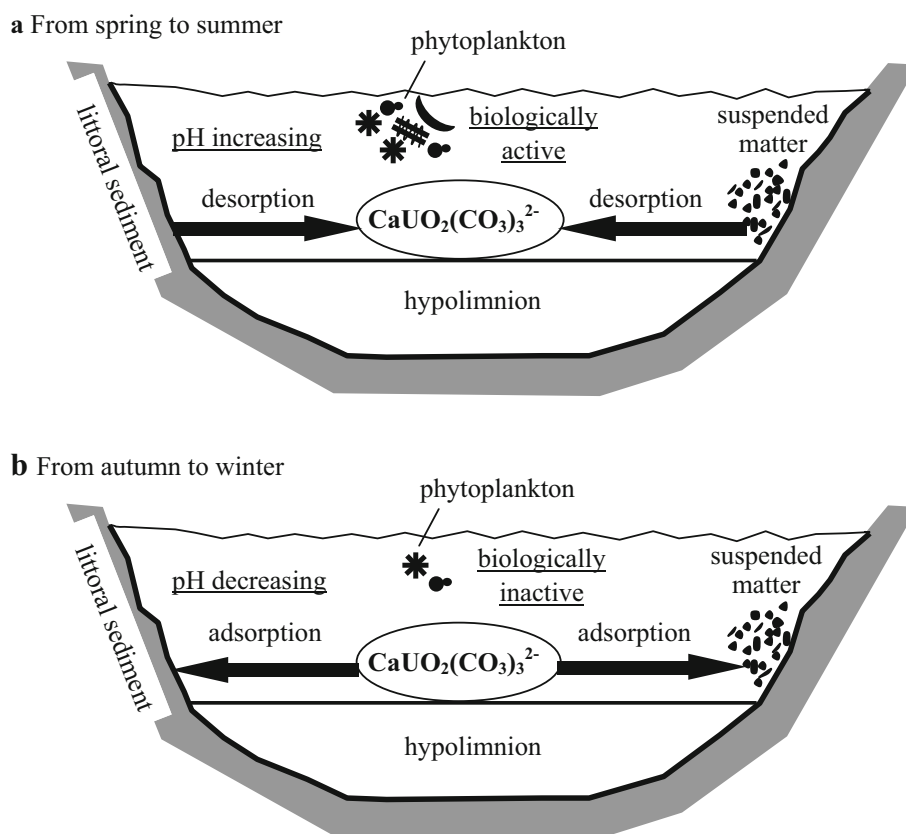
were 6.00×10^3 pmol m^{-2} day^{-1} in 2011 and 1.10×10^4 pmol m^{-2} day^{-1} in 2012. Although the adsorption rate in 2011 is slightly lower, these values are of the same order of magnitude as the rates of U release and assimilation observed experimentally (1.86×10^4 and 2.76×10^4 pmol m^{-2} day^{-1}, respectively; Fig. 6). Therefore, we conclude that the seasonal variation in dissolved U concentration in the epilimnion mainly results from the desorption/adsorption of U from/onto the littoral sediment in response to variation in water pH, as shown experimentally.

Both of the estimated desorption and adsorption rates in 2012 are approximately 1.9 times greater than those in 2011. Since the pH during summer was much higher in 2012 (maximum: 9.6) than in 2011 (maximum: 8.0), the amount of U desorbed from the solid phase in response to the pH increase was possibly greater in 2012. Similarly, the amount of U adsorbed onto the solid phase from autumn to winter was greater in 2012 because the pH decreased more significantly in that year (Table 3).

The simulated U concentrations were slightly lower than the measured values in autumn (Fig. 8), suggesting that there are some additional inputs of U to the lake water during these periods. A possible source of these inputs is the release of U from the sediment at approximately 5–30 m depths. As the thermocline becomes deeper during autumn, the upper part of the hypolimnion is taken into the epilimnion and the pH of that layer increases. For example,

the pH at 25 m depth increased from 6.9 in September to 7.2 in December 2012 (data not shown). In response to such pH increase, U is expected to be desorbed from the sediment in contact with the water layer newly taken from the hypolimnion into the epilimnion. However, it is difficult to incorporate such U desorption into the model, because it is almost impossible to predict the area and the period in which U is desorbed from the sediment newly contacting the epilimnion.

Another possible source is suspended particulate matter, which is supplied abundantly from the watershed to the lake in autumn as a result of typhoons. For example, very high concentrations of suspended particulate matter of 10.4 and 10.0 mg l^{-1} were observed in the epilimnion of the northern basin in September 2011 and 2012, respectively, compared to its usual concentrations of around 1 mg l^{-1} in summer and winter (Shiga Prefecture 2012, 2013). Therefore, it is inferred that much U was released from this suspended particulate matter in autumn.

Conclusions and implications

Our study revealed seasonal variation in dissolved U concentration in the well-oxygenated epilimnion of Lake Biwa; it started to increase in spring, peaked in summer, and decreased from autumn to winter. Such behavior

differs from the commonly accepted view that U shows conservative behavior in oxygenated seas (Ku et al. 1977; Delanghe et al. 2002) and lakes (Falkner et al. 1991). In addition, our results show that the solid phase behaves as both source and sink of U, according to variation in water pH. Although a number of experimental studies have revealed the adsorptive properties of (calcium–)uranyl-carbonate complexes onto the solid phase, to our knowledge this is the first study to report that such adsorptive behavior of U in response to pH variation controls the geochemical dynamics of U in natural waters. The present findings suggest that U in natural waters shows more complicated behavior than anticipated, and therefore further investigations will help to improve the understanding of U geochemistry.

Our findings also have implications for understanding the transport and distribution of anthropogenic U in aquatic environments, particularly in limnetic areas. If natural water in a slightly acidic or neutral pH range is contaminated by anthropogenic U, for example, a large proportion of the U is expected to be retained in the solid phase. However, our findings suggest that the adsorbed U is desorbed from the solid phase in response increase in pH to the alkaline range, resulting in increased concentration of dissolved U. This seems to occur in the epilimnion of mesotrophic or eutrophic lakes and in oxygenated estuaries, where river water mixes with seawater of higher pH and alkalinity.

References

Anderson RF, Fleisher MQ, Lehuray AP (1989) Concentration, oxidation state, and particulate flux of uranium in the Black Sea. Geochim Cosmochim Acta 53:2215–2224

Barnett MO, Jardine PM, Brooks SC (2002) U (VI) adsorption to heterogeneous subsurface media: application of a surface complexation model. Environ Sci Technol 36:937–942

Bernhard G, Geipel G, Reich T, Brendler V, Amayti S, Nistche H (2001) Uranyl (VI) carbonate complex formation: validation of the $Ca_2UO_2(CO_3)_3$ (aq.) species. Radiochim Acta 89:511–518

Broecker WS, Peng TH (1982) Reactive metals and the great particulate sweep. In: Broecker WS, Peng TH (eds) Tracers in the sea. Lamont-Doherty Geol Obs, New York, pp 166–235

Chabaux F, Riotte J, Clauer N, France-Lanord C (2001) Isotopic tracing of the dissolved U fluxes of Himalayan rivers: implications for present and past U budgets of the Ganges-Brahmaputra system. Geochim Cosmochim Acta 65:3201–3217

Chabaux F, Bourdon B, Riotte J (2008) U-series geochemistry in weathering profiles, river waters and lakes. In: Krishnaswami S, Cochran JK (eds) U/Th series radionuclides in aquatic systems. Elsevier, Amsterdam, pp 49–104 (**Radioactivity in the environment, Vol 13**)

Delanghe D, Bard E, Hamelin B (2002) New TIMS constraints on the uranium-238 and uranium-234 in seawaters from the main ocean basins and the Mediterranean Sea. Mar Chem 80:79–93

Dong W, Brooks SC (2006) Determination of the formation constants of ternary complexes of uranyl and carbonate with alkaline earth metals (Mg^{2+}, Ca^{2+}, Sr^{2+}, and Ba^{2+}) using anion exchange method. Environ Sci Technol 40:4689–4695

Dong W, Ball WP, Liu C, Wang Z, Stone AT, Bai J, Zachara JM (2005) Influence of calcite and dissolved calcium on uranium (VI) sorption to a Hanford subsurface sediment. Environ Sci Technol 39:7949–7955

Falkner KK, Measures CI, Herbelin SE, Edmond JM (1991) The major and minor element geochemistry of Lake Baikal. Limnol Oceanogr 36:413–423

Fox PM, Davis JA, Zachara JM (2006) The effect of calcium on aqueous uranium (VI) speciation and adsorption to ferrihydrite and quartz. Geochim Cosmochim Acta 70:1379–1387

Fujinaga T, Hori T (1982) Chemical dynamics in Lake Biwa. In: Fujinaga T, Hori T (eds) Environmental chemistry on Lake Biwa. Japan Society for the Promotion of Science, Tokyo, pp 27–111 (**in Japanese**)

Harita Y, Hori T, Sugiyama M (2005) Release of trace oxyanions from littoral sediments and suspended particles induced by pH increase in the epilimnion of lakes. Limnol Oceanogr 50:636–645

Ho CH, Miller NH (1986) Adsorption of uranyl species from bicarbonate solution onto hematite particles. J Colloid Interface Sci 110:165–171

Horie S (1961) Paleolimnological problems of Lake Biwa-ko. Mem Coll Sci Univ Kyoto Ser B 28:53–71

Hsi CKD, Langmuir D (1985) Adsorption of uranyl onto ferric oxyhydroxides: application of the surface complexation site-binding model. Geochim Cosmochim Acta 49:1931–1941

Ishibashi M, Fujinaga T, Kuwamoto T, Ogino Y (1967) Chemical studies of the ocean. XCIX: coprecipitation of uranium (VI) with ferric hydroxide. J Chem Soc Jpn 88:73–76 (**in Japanese**)

Kalmykov SN, Choppin GR (2000) Mixed $Ca^{2+}/UO_2^{2+}/CO_3^{2-}$ complex formation at different ionic strength. Radiochim Acta 88:603–606

Klinkhammer GP, Palmer MR (1991) Uranium in the oceans: where it goes and why. Geochim Cosmochim Acta 55:1799–1806

Ku TL, Knauss KG, Mathieu GG (1977) Uranium in open ocean: concentration and isotopic composition. Deep-Sea Res 24:1005–1017

Kunimatsu T (1981) Water quality of the river water, groundwater and rain water in the catchment area and outflow water of Lake Biwa. Kankyokagaku Res Report B105:82–105 (**in Japanese**)

Langmuir D (1978) Uranium solution-mineral equilibria at low temperatures with applications to sedimentary ore deposits. Geochim Cosmochim Acta 42:547–569

Mito S, Sohrin Y, Norisuye K, Matsui M, Hasegawa H, Maruo M, Tsuchiya M, Kawashima M (2004) The budget of dissolved trace metals in Lake Biwa, Japan. Limnology 5:7–16

Mochizuki A, Sugiyama M (2012) Natural background concentration of dissolved uranium in Japanese rivers. Jpn J Limnol 73:89–107 (**in Japanese**)

Okamoto I (1992) Seasonal variation in water temperature. In: Okamoto I (ed) The investigation of Lake Biwa. Jinbunshoin, Kyoto, pp 32–52 (**in Japanese**)

Pabalan RT, Turner DR (1997) Uranium (+6) sorption on montmorillonite: experimental and surface complexation modeling study. Aquat Geochem 2:203–226

Ryu JS, Lee KS, Chang HW, Cheong CS (2009) Uranium isotopes as a tracer of sources of dissolved solutes in the Han River, South Korea. Chem Geol 258:354–361

Sakamoto H, Yamamoto K, Shirasaki T, Yamazaki H (2004) Determination of U and major elements in Lake Biwa water and its inflow river water by ICP/three dimensional quadrupole mass spectrometer. Bunseki Kagaku 53:91–99 (in Japanese)

Schecher WD, McAvoy DC (2006) MINEQL+: a chemical equilibrium modeling system (ver. 4.6). Environmental Research Software, Hallowell, ME

Shiga Prefecture (2012) Water quality at respective depth in Lake Biwa. In: Shiga Prefecture (eds) Environments in Shiga 2012. Shiga Prefecture, Shiga, pp 135–176 (in Japanese)

Shiga Prefecture (2013) Water quality at respective depth in Lake Biwa. In: Shiga Prefecture (eds) Environments in Shiga 2013. Shiga Prefecture, Shiga, pp 133–174 (in Japanese)

Somiya I (2000) Lake Biwa. Gihodo (in Japanese)

Stewart BD, Mayes MA, Fendorf S (2010) Impact of uranyl–calcium-carbonato complexes on uranium (VI) adsorption to synthetic and natural sediments. Environ Sci Technol 44:928–934

Stumm W, Morgan JJ (1996) Aquatic chemistry. Wiley, Hoboken

Sugiyama M (1989) Seasonal variation of vanadium concentration in Lake Biwa, Japan. Geochem J 23:111–116

Sugiyama M, Hori T, Kihara S, Matsui M (2005) Geochemical behavior of trace elements in Lake Biwa. Limnology 6:117–130

Takaku Y, Akiba S, Hayashi T, Kano M, Ohtsuka Y (2003) Development of "all-ium" analytical method for water samples at Lake Biwa. In: Holland JG, Tanner SD (eds) Plasma source mass spectrometry. The Royal Society of Chemistry, London, pp 105–111

Takamatsu T, Kawashima M, Matsushita R, Koyama M (1985) General distribution profiles of thirty-six elements in sediments and manganese concretions of Lake Biwa. Jpn J Limnol 46:115–127

Van der Weijden CH, Middelburg JJ, De Lange GJ, Van der Sloot HA, Hoede D, Woittiez JRW (1990) Profiles of the redox-sensitive trace elements As, Sb, V, Mo and U in the Tyro and Bannock Basins (eastern Mediterranean). Mar Chem 31:171–186

Waite TD, Davis JA, Payne TE, Waychunas GA, Xu N (1994) Uranium (VI) adsorption to ferrihydrite: application of a surface complexation model. Geochim Cosmochim Acta 58:5465–5478

Wang Z, Zachara JM, Yantasee W, Gassman PL, Liu C, Joly AG (2004) Cryogenic laser induced fluorescence characterization of U (VI) in Hanford vadose zone pore waters. Environ Sci Technol 38:5591–5597